Investigation of Three Immiscible Fluids in a Microchannel Accounting for the Pressure Gradient and the Electroosmotic Flow

Nicolas La Roche-Carrier, Guyh Dituba Ngoma, Fouad Erchiqui and Ibrahim Hamani

School of Engineering's Department, University of Quebec in Abitibi-Témiscamingue,
445, Boulevard de l'Université, Rouyn-Noranda, Quebec, J9X 5E4, Canada

Keywords: Immiscible Fluids, Microchannel, Modeling and Simulation.

Abstract: This study deals with the investigation of three immiscible fluids in a microchannel consisting of two parallel plates. These fluids were composed of two electric conducting fluids and one electric nonconducting fluid. The concept of pumping a nonconducting fluid using interfacial viscous shear stress was applied accounting for the effect of the electroosmosis and pressure gradient. The electric potential and the flow parameters were found resolving the Poisson-Boltzmann equation and the modified Navier-Stokes equations for a hydraulic steady fully-developed laminar flow of an incompressible fluid. The results achieved revealed the influence of the wall and interfacial zeta potentials, the pressure difference, and the dynamic fluid viscosity ratio on the flow characteristics of the three immiscible fluids. The developed approach was compared with a model of two immiscible flows to highlight the relevance of this work.

1 INTRODUCTION

Microfluidic transport is widely used in the fields of micropumps, micropower generation, chemical processes, biomechanical processes and heat transfer, where surface effects dominate the flow behavior within microdevices (Dituba Ngoma G. et al., 2005). The precise knowledge of the immiscible fluids flow behavior in microchannels is essential to develop high-performance microfluidic devices to pump a nonconducting fluid by means of conducting fluids. This can be achieved taking relevant fluid parameters and microchannel configurations into consideration in the planning, design and optimization phases. Most previous investigations of pressure gradient and electroosmotic flow in microchannels were performed using a single conducting fluid with the zeta potentials at the microchannel walls (Dhinakaran S. et al., 2010; Vainshtein P. et al., 2002; and Brask A. et al., 2005). There, the effects of surface potential, electric field, ionic concentration and channel size on the velocity distribution and the effect of friction on flow characteristics. Furthermore, Yong et al., 2011 numerically analyzed the immiscible kerosene-water two-phase flows in microchannels connected by a T-junction using lattice Boltzmann method. In addition, Dituba Ngoma G. et al., 2005; and Gao Y. et al., 2005,

conducted a study on two immiscible fluids consisting of a conducting fluid and a nonconducting fluid in a microchannel. The electric field and the pressure gradient were applied. Moreover, an analytical model of mixed electroosmotic/pressure driven three immiscible fluids in a rectangular microchannel was developed by Li H. et al., 2009. They analyzed the effects of viscosity ratio, electroosmosis and pressure gradient on velocity profile and flow rate. Thorough analysis of previous works clearly demonstrated that the research results obtained are specific to the microchannel configuration depending on considered key parameters of fluids and microchannels. Therefore, in this work, to enhance the fluid flow of nonconducting fluids and performances of the flow in microchannels, an investigation was conducted considering the fluid flow of the three immiscible fluids in a two parallel plates to deeply analyze the impacts of the zeta potential, the pressure difference and the dynamic viscosity on the flow characteristics of the three fluids.

2 MATHEMATICAL FORMULATION

The model of three immiscible fluids in two parallel plates considered in this study is shown in Fig. 1. The two plates separated by a distance h. The microchannel is filled of two electric conducting fluids, the fluid 1 and the fluid 3, and one non-conducting fluid, the fluid 2. These fluids have different dynamic viscosities which are specified by μ_1, μ_2, and μ_3, respectively. The interface positions are specified using the heights h_1 and h_2. The forces acting on the conducting fluids include the pressure force and the electric body force generated by the double layer electric field. For the non-conducting fluid, only the pressure force acts on this.
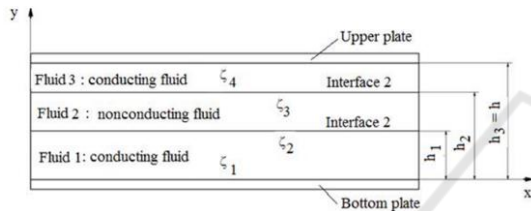

Figure 1: Model of three immiscible fluids.

To develop the governing equations for the liquid flow of the three immiscible fluids in a microchannel accounting for the electroosmosis, the following assumptions were made: (i) A steady state, one-dimensional and laminar flow was assumed; (ii) no-slip boundary conditions were assumed; (iii) a planar interface between the immiscible fluids was assumed; (iv) the fluid shear stress and the flow velocity were the same at the fluid interface; (v) the fluids were assumed to be incompressible; and (vi) the gravity effect was negligible.

2.1 Electric Potential Field

According to the electrokinetic (Dituba Ngoma G. et al., 2005; and Li H. et al., 2009), the equation of the electric potential of ions, ϕ, in y direction for the conducting fluids is given as:

$$\frac{d^2\phi}{dy^2} = -\frac{\rho_e}{\varepsilon\varepsilon_0}. \tag{1}$$

where ε is the dielectric constant of the solution, ε_0 the permittivity of vacuum, and ρ_e the net charge density.

The net charge density can be written assuming a symmetric electrolyte as:

$$\rho_e = -2n_\infty z_0 e \sinh\left(\frac{z_0 e}{k_b T}\phi\right), \tag{2}$$

where e, k_b, n_∞, T and z_0 are the elementary charge, Boltzmann constant, bulk concentration of ions, absolute temperature and valence of ions, respectively.

Combining the Eqs. 1 and 2, and using the Debye-Hückel approximation, Eq. 3 is found:

$$\frac{d^2\phi}{dy^2} = \kappa^2\phi, \tag{3}$$

where $\kappa = z_0 e \sqrt{\dfrac{2n_\infty}{\varepsilon\varepsilon_0 k_b T}}$ is the Debye-Hückel parameter and $\dfrac{1}{\kappa}$ is the Debye length.

The net charge density Eq. 2 can be rewritten as:

$$\rho_e = \frac{-2n_\infty z_0^2 e^2}{k_b T}\phi. \tag{4}$$

Introducing the Debye-Hückel parameter in Eq. 4, the last can be expressed by:

$$\rho_e = -\varepsilon\varepsilon_0 \kappa^2\phi. \tag{5}$$

To solve Eq. 3, the following boundary conditions for the conducting fluids are used:

$$
\begin{aligned}
y = 0 \quad &\phi = \zeta_1 \text{ for the bottom wall,}\\
y = h_1 \quad &\phi = \zeta_2 \text{ for the interface of the fluids}\\
&\quad \text{1 and 2,}\\
y = h_2 \quad &\phi = \zeta_3 \text{ for the interface of the}\\
&\quad \text{fluids 2 and 3,}\\
y = h_3 \quad &\phi = \zeta_4 \text{ for the upper wall.}
\end{aligned} \tag{6}
$$

Using the dimensionless parameters and variables, Eq. 3 can be formulated as:

$$\frac{d^2\phi^*}{dy^{*2}} = K^2\phi^*. \tag{7}$$

where $\phi^* = \dfrac{z_0 e\phi}{k_b T}$, $y^* = \dfrac{y}{h}$, $K = \kappa h$, h is the distance between the plates, it equal to h_3.

The boundary conditions of Eq. (7) in dimensionless form can be written as for the conducting fluid "fluid 1":

$$
\begin{aligned}
y^* = 0 \quad &\phi^* = \zeta_1^*,\\
y^* = h_1^* \quad &\phi^* = \zeta_2^*.
\end{aligned} \tag{8}
$$

For the conducting fluid "fluid 3". They are expressed by:

$$
\begin{aligned}
y^* = h_2^* \quad &\phi^* = \zeta_3^*,\\
y^* = h_3^* = 1 \quad &\phi^* = \zeta_4^*.
\end{aligned} \tag{9}
$$

Where $h_1{}^* = \dfrac{h_1}{h}$, $h_2{}^* = \dfrac{h_2}{h}$, $h_3{}^* = \dfrac{h_3}{h} = 1$, $\zeta_1{}^* = \dfrac{z_0 e \zeta_1}{k_b T}$,

$\zeta_3{}^* = \dfrac{z_0 e \zeta_3}{k_b T}$, $\zeta_4{}^* = \dfrac{z_0 e \zeta_4}{k_b T}$.

In addition, the net charge density in dimensionless form is given by:

$$\rho_e{}^* = \frac{\rho_e}{n_\infty z_0 e} . \qquad (10)$$

When considering the expression of ϕ^*, Eq. 10 becomes:

$$\rho_e{}^* = -2\phi^* . \qquad (11)$$

The solutions of Eqs. 7 and 11 can be written as:

$$\begin{aligned} \phi^* &= A e^{Ky^*} + B e^{-Ky^*}, \\ \rho_e^* &= 2\left(A e^{ky^*} + B e^{-Ky^*} \right) \end{aligned} \qquad (12)$$

where A and B are determined accounting for the boundary conditions. In general case, these boundary conditions can be expressed as follows:

$$\begin{aligned} y^* &= h_i^* & \phi^* &= \zeta_i{}^*, \\ y^* &= h_j^* & \phi^* &= \zeta_j{}^* . \end{aligned} \qquad (13)$$

Substituting Eq. 13 for ϕ^* in Eq. 12, Eq. 14 is found

$$\begin{aligned} \varsigma_i^* &= A e^{Kh_i^*} + B e^{-Kh_i^*}, \\ \varsigma_j^* &= A e^{Kh_j^*} + B e^{-Kh_j^*} . \end{aligned} \qquad (14)$$

From Eq. 14, A and B are determined:

$$A = \frac{\varsigma_i e^{-Kh_j^*} - \varsigma_j e^{-Kh_i^*}}{e^{K(h_i^* - h_j^*)} - e^{-K(h_i^* - h_j^*)}},$$

$$B = \frac{\varsigma_i e^{Kh_j^*} - \varsigma_j e^{Kh_i^*}}{e^{-K(h_i^* - h_j^*)} - e^{K(h_i^* - h_j^*)}} . \qquad (15)$$

Furthermore, for the conducting fluids "fluid 1" and "fluid 2", A and B are calculated using Eq. 16:

$$\begin{aligned} h_i^* &= 0 & \zeta_i{}^* &= \zeta_1{}^*, \\ h_j^* = h_1^* \ h_i^* &= h_2^* \ h_j^* = 1 & \zeta_j{}^* &= \zeta_2{}^*, \ \zeta_i{}^* = \zeta_3{}^*, \\ & & \zeta_j{}^* &= \zeta_4{}^* . \end{aligned} \qquad (16)$$

2.2 Hydrodynamic Field

The modified Navier-Stokes equations for the fluids 1, 2, and 3 can be expressed by:

$$0 = P_x + \mu_3 \frac{\partial^2 u_3}{\partial y^2} + E\rho_e,$$

$$0 = P_x + \mu_1 \frac{\partial^2 u_1}{\partial y^2} + E\rho_e, \qquad (17)$$

$$0 = P_x + \mu_2 \frac{\partial^2 u_2}{\partial y^2} .$$

where $P_x = -\dfrac{dp}{dx}$ assuming that the pressure gradient in x direction is constant. E and $E\rho_e$ are the electric field and the electric body force, respectively.

Eq. 17 represents three second-order differential equations. Thus, six boundary conditions are required in order to solve them. The no-slip boundary conditions can be written as based on Fig.1:

$$\begin{aligned} u_1(y = 0) &= 0, \\ u_3(y = h_3) &= 0 . \end{aligned} \qquad (18)$$

Moreover, the boundary conditions for the same velocity at the interfaces of the fluids 1 and 2, and the fluids 2 and 3 can be formulated as follows:

$$\begin{aligned} u_1(y = h_1) &= u_2(y = h_1), \\ u_2(y = h_2) &= u_3(y = h_2) . \end{aligned} \qquad (19)$$

In addition, the boundary conditions for the interfacial shear stresses are described as:

$$\mu_1 \frac{\partial u_1}{\partial y}\bigg|_{y=h_1} = \mu_2 \frac{\partial u_2}{\partial y}\bigg|_{y=h_1},$$

$$\mu_2 \frac{\partial u_2}{\partial y}\bigg|_{y=h_2} = \mu_3 \frac{\partial u_3}{\partial y}\bigg|_{y=h_2} . \qquad (20)$$

Solving Eq. 17 accounting for the boundary conditions, the dimensionless velocities are determined:

$$u_1^* = -\frac{C_0 y^{*2}}{2} + C_1 \phi^* + a_1 y^* + a_2,$$

$$u_2^* = -\frac{C_4 y^{*2}}{2} + b_1 y^* + b_2, \qquad (21)$$

$$u_3^* = -\frac{C_2 y^{*2}}{2} + C_3 \phi^* + a_3 y^* + a_4 .$$

where $u_1^* = \dfrac{u_1}{u_0}$, $u_2^* = \dfrac{u_2}{u_0}$, $u_3^* = \dfrac{u_3}{u_0}$, u_0 is an arbitrary reference velocity,

$C_0 = \dfrac{h^2 P_x}{\mu_1 u_0}$, $C_1 = \dfrac{u_{h1}}{u_0}$, $C_2 = \dfrac{h^2 P_x}{\mu_3 u_0}$, $C_3 = \dfrac{u_{h3}}{u_0}$, and

$C_4 = \dfrac{h^2 P_x}{\mu_2 u_0}$. u_{h1} and u_{h3} are the Helmholtz-

Smoluchowski electroosmotic velocities for the conducting fluids "fluid 1" and "fluid 3", respectively. They are given by:

$$u_{h1} = \frac{E\varepsilon\varepsilon_0 K_b T}{z_0 e\mu_1} \quad \text{and} \quad u_{h3} = \frac{E\varepsilon\varepsilon_0 K_b T}{z_0 e\mu_3} . \qquad (22)$$

The dimensionless boundary conditions can be formulated as:

$$u_1^*(y^* = 0) = 0,$$

$$u_1^*\left(h_1^*\right) = u_2^*\left(h_1^*\right),$$

$$u_2^*\left(h_2^*\right) = u_3^*\left(h_2^*\right),$$

$$u_3^*\left(h_3^* = 1\right) = 0, \qquad (23)$$

$$\left.\frac{\partial u_1^*}{\partial y^*}\right|_{y^*=h_1^*} = \alpha \left.\frac{\partial u_2^*}{\partial y^*}\right|_{y^*=h_1^*},$$

$$\alpha \left.\frac{\partial u_2^*}{\partial y^*}\right|_{y^*=h_2^*} = \beta \left.\frac{\partial u_3^*}{\partial y^*}\right|_{y^*=h_2^*},$$

where $\alpha = \dfrac{\mu_2}{\mu_1}$ and $\beta = \dfrac{\mu_3}{\mu_1}$.

Accounting for the boundary conditions Eq. 23, the system of six equations in matrix form are found in order to determine the constants a_1, a_2, a_3, a_4, b_1 and b_2:

$$\begin{pmatrix} 0 & 1 & 0 & 0 & 0 & 0 \\ 0 & 0 & 1 & 1 & 0 & 0 \\ h_1^* & 1 & 0 & 0 & -h_1^* & -1 \\ 0 & 0 & h_2^* & 1 & -h_2^* & -1 \\ 1 & 0 & 0 & 0 & -\alpha & 0 \\ 0 & 0 & \beta & 0 & -\alpha & 0 \end{pmatrix} \begin{pmatrix} a_1 \\ a_2 \\ a_3 \\ a_4 \\ b_1 \\ b_2 \end{pmatrix} = \begin{pmatrix} G_1 \\ G_2 \\ G_3 \\ G_4 \\ G_5 \\ G_6 \end{pmatrix}, \qquad (24)$$

$$\text{6x6} \qquad\qquad \text{6x1} \quad\ \text{6x1}$$

where:

$$G_1 = -C_1 \zeta_1^*,$$

$$G_2 = \frac{C_2}{2} - C_3 \zeta_4^*,$$

$$G_3 = \frac{C_0 h_1^{*2}}{2} - C_1 \zeta_2^* - \frac{C_4 h_1^{*2}}{2},$$

$$G_4 = \frac{C_2 h_2^{*2}}{2} - C_3 \zeta_3^* - \frac{C_4 h_2^{*2}}{2}, \qquad (25)$$

$$G_5 = -\alpha C_4 h_1^* + C_0 h_1^*$$
$$\qquad - KC_1\left(A_1 e^{Kh_1^*} - B_1 e^{-Kh_1^*}\right),$$

$$G_6 = \beta C_2 h_2^* - \alpha C_4 h_2^*$$
$$\qquad - \beta KC_3\left(A_3 e^{Kh_2^*} - B_3 e^{-Kh_2^*}\right).$$

2.3 Dimensionless Flow Rates

The flow rate between the parallel plates is determined by integrating the flow velocity distribution over the cross-sectional area. For the fluids 1, 2, and 3, the dimensionless flow rates are expressed respectively by:

$$Q_1^* = -\frac{C_0}{6} h_1^{*3} + \frac{a_1}{2} h_1^{*2} + a_2 h_1^*$$
$$\qquad + \frac{C_1}{K}\left(A_1\left(e^{Kh_1^*} - 1\right) - B_1\left(e^{-Kh_1^*} - 1\right)\right),$$

$$Q_2^* = -\frac{C_4\left(h_2^{*3} - h_1^{*3}\right)}{6} + b_1\left(\frac{h_2^{*2} - h_1^{*2}}{2}\right) \qquad (26)$$
$$\qquad + b_2\left(h_2^* - h_1^*\right),$$

$$Q_3^* = -\frac{C_2}{6}\left(1 - h_2^{*3}\right) + \frac{a_3}{2}\left(1 - h_2^{*2}\right) + a_4\left(1 - h_2^*\right)$$
$$\qquad + \frac{C_3}{K}\left(A_3\left(e^K - e^{Kh_2^*}\right) - B_3\left(e^{-K} - e^{-Kh_2^*}\right)\right).$$

3 NUMERICAL RESULTS AND DISCUSSION

Numerical simulations were done using the MATLAB software to investigate and analyze the effects of the wall and interfacial zeta potentials, the pressure difference, the interface position, the dynamic viscosity ratio on flow characteristics of the three immiscible fluids in a microchannel between two plates. The main reference data for all simulation runs in this study are given as: $\varepsilon_0 = 8.854 \times 10^{-12}$ C/(m V), $\varepsilon = 80$, $n_\infty = 6.022 \times 10^{20}$ 1 m³, $z_{0=1}$, E =15000 V/m , T = 298 K, $k_b = 1.381 \times 10^{-23}$ J/K, $\mu_1 = 0.001$ Pa s, $\alpha = 1$, $\beta = 1$, L = 0.02 m, and $u_0 = 1$ m/s.

3.1 Impact of the Zeta Potential

To analyze the impact of the zeta potential on the electric potential for the conducting fluids "fluid 1" and "fluid 3", all parameters were kept constant except the wall, and interfacial zeta potentials. Fig. 2 shows the dimensionless electric potential as a function of the dimensionless height of the fluid with the dimensionless wall and the interfacial zeta potentials as parameters. There, it can be seen that the effect of the zeta potential is very pronounced on the microchannel bottom and upper walls, and the interface positions of the three fluids. The electric potential is zero for the nonconducting "fluid 2".
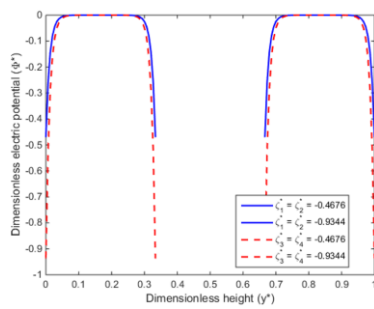
Figure 2: Dimensionless electric potential versus dimensionless height.

3.2 Impact of the Pressure Difference

To investigate the impact that the pressure difference in a microchannel has on the flow velocity, the dynamic viscosity ratios, the wall zeta potentials, the interfacial zeta potentials, the interface positions; the pressure differences were varied using the dimensionless values. Fig. 3 shows the dimensionless flow velocity distribution in the microchannel cross-section. From this figure, it can be observed that the dimensionless flow velocities for the three immiscible fluids increase when the dimensionless pressure difference between the microchannel inlet and outlet increases. This well explain the pumping of the nonconducting fluid "fluid 2" by means of two conducting fluids "fluid 1" and "fluid 3".
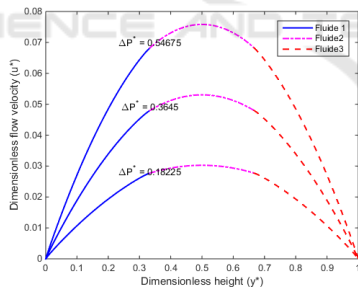

Figure 3: Dimensionless flow velocity versus dimensionless height.

Moreover, Fig. 4 represents the dimensionless interfacial flow velocity for the three fluids as a function of the dimensionless pressure difference, where it can be seen that the dimensionless interfacial flow velocity increases with the dimensionless pressure difference.
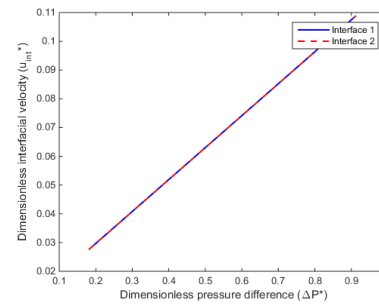

Figure 4: Dimensionless interfacial flow velocity versus dimensionless pressure difference.

3.3 Impact of the Dynamic Viscosity Ratio

To examine the effect of the dynamic viscosity ratio "α" between the fluids 1 and 2 on the interfacial flow velocity, and the flow velocity; all parameters were kept constant, except the dynamic viscosity ratio "α". Fig. 5 shows the distribution of the dimensionless flow velocity for the three fluids as a function of the dimensionless height of the fluid with the dynamic velocity ratio "α" as parameter. From this figure, it can be seen that the dimensionless flow velocities for the three fluids decrease when the dynamic viscosity ratio "α" increases. This can be explained by the fact that the resistance to fluid flow increases when the dynamic viscosity of a fluid increases.

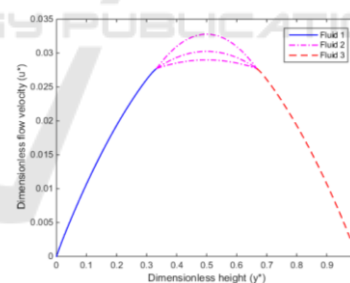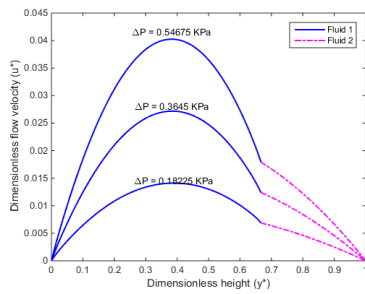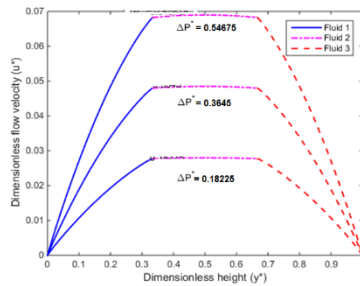Figure 5: Dimensionless flow rate versus dimensionless height.

3.4 Model Comparison

The developed model of the three immiscible fluids in microchannel consisting of two parallel plates was compared with the model of two immiscible fluids in two parallel plates (Dituba Ngoma G. et al., 2005). The results obtained shows that the maximum dimensionless velocity was achieved for the model of three fluids as depicted in Fig. 6. That highlights the relevance to consider the concept of two conducting fluids to drive a conducting fluid.

a) Model of two immiscible fluids

b) Model of three immiscible fluids

Figure 6: Model comparison.

4 CONCLUSION

In this work, a model of the flow of three immiscible fluids in a microchannel formed by two parallel plates was investigated. The concept of pumping an electric nonconducting fluid using two electric conducting fluids was applied. The combined effect of the pressure gradient and electroosmosis was accounted for to identify the flow parameters that improve the flow of the nonconducting fluid. Based on the modified Navier-Stokes and the Poisson-Boltzmann equations, numerical simulations were accomplished. The results obtained demonstrate that, among other things, the dynamic viscosity ratios, the zeta potentials and the pressure difference affects the flow behavior in a microchannel in a strong yet different manner. A comparison between the developed approach of three fluids and a model of two fluids was done to show the relevance of this study.

REFERENCES

Dhinakaran S., Afonso A.M., Alves M.A., Pinho F.T. 2010. Steady viscoelastic fluid flow between parallel plates under electro-osmotic forces: Phan-Thien–Tanner model. *Journal of Colloid and Interface Science* 344, 513–520.

Vainshtein P. and Gutfinger C. 2002. On electroviscous effects in microchannels. *J. Micromech. Microeng*. 12, 252-256.

Brask A., Goranovic G., Jensen M. J. and Bruus H., A, 2005. Novel electro-osmotic pump design for nonconducting liquids: theoretical analysis of flow rate–pressure characteristics and stability, J. *Micromech. Microeng.* 15, 883-891.

Yong Y., Yang C., Jiang Y., Joshi A., Shi Y. and Yin X., 2011. Numerical simulation of immiscible liquid-liquid flow in microchannels using lattice Boltzmann method. *Science China Chemistry*, Vol.54 No.1: 244–256.

Gao Y., Wong T. N., Yang C., Ooi K. T., 2005. Two-fluid electroosmotic flow in microchannels. Journal of Colloid and Interface Science 284 (2005) 306-314.

Dituba Ngoma G., Erchiqui Fouad, 2005. Pressure gradient and electroosmotic effects on two immiscible fluids in a microchannel between two parallel plates, *Journal of Micromechanics and Microengineering* 16, 83–91.

Li H., Teck N. W., Nam-Trung N., 2009. Analytical model of mixed electroosmotic/pressure driven three immiscible fluids in a rectangular microchannel. *International Journal of Heat and Mass Transfer* 52, 4459-4469.